


ARTICLE

Thermodynamic Models of the Fluid $\text{H}_2\text{O}-\text{CO}_2-\text{NaCl}-\text{CaCl}_2$ and Its Ternary Subsystems for Temperatures of 150–350 °C and Pressures of 0.2–1.4 kbar

Mikhail V. Ivanov 

Institute of Precambrian Geology and Geochronology Russian Academy of Sciences, nab. Makarova 2, St. Petersburg 199034, Russia

ABSTRACT

Numerical thermodynamic models are proposed for the quaternary fluid system $\text{H}_2\text{O}-\text{CO}_2-\text{NaCl}-\text{CaCl}_2$ and its ternary subsystems $\text{H}_2\text{O}-\text{NaCl}-\text{CaCl}_2$, $\text{H}_2\text{O}-\text{CO}_2-\text{NaCl}$, and $\text{H}_2\text{O}-\text{CO}_2-\text{CaCl}_2$. The models are valid for temperatures from 150 °C to 350 °C, pressures from 0.2 to 1.4 kbar, and for arbitrary concentrations of salts. The latter feature is inherited from the earlier developed models of binary systems $\text{H}_2\text{O}-\text{NaCl}$ and $\text{H}_2\text{O}-\text{CaCl}_2$. All the models are formulated in terms of the Gibbs free energy. The entropy term in the equation for the Gibbs free energy of mixing is introduced in a general form, based on the number of different ways of arranging particles in the system that lead to the same total energy. The parameters of the energy terms corresponding to the interactions of particles in binary and ternary subsystems are obtained by fitting published experimental data. The concentrations of salts in the gas phase are simulated based on the salt evaporation free energy. Our model, also available as a computer code, makes it possible to predict the physicochemical properties of fluids involved in hydrothermal processes in the upper crust: the phase state of the system (homogeneous or two-phase fluid), activities of the components, densities, and compositions of the (coexisting) fluid phases. The model offers a numerical tool for analyzing fluid inclusion data and better understanding of metamorphic and metasomatic processes in the upper

*CORRESPONDING AUTHOR:

Mikhail V. Ivanov, Institute of Precambrian Geology and Geochronology Russian Academy of Sciences, nab. Makarova 2, St. Petersburg 199034, Russia; Email: mikhail.v.ivanov52@gmail.com

ARTICLE INFO

Received: 8 August 2025 | Revised: 22 September 2025 | Accepted: 25 September 2025 | Published Online: 24 October 2025
DOI: <https://doi.org/10.30564/jees.v7i10.11540>

CITATION

Ivanov, M.V., 2025. Thermodynamic Models of the Fluid $\text{H}_2\text{O}-\text{CO}_2-\text{NaCl}-\text{CaCl}_2$ and Its Ternary Subsystems for Temperatures of 150–350 °C and Pressures of 0.2–1.4 kbar. *Journal of Environmental & Earth Sciences*. 7(10): 51–68. DOI: <https://doi.org/10.30564/jees.v7i10.11540>

COPYRIGHT

Copyright © 2025 by the author(s). Published by Bilingual Publishing Group. This is an open access article under the Creative Commons Attribution-NonCommercial 4.0 International (CC BY-NC 4.0) License (<https://creativecommons.org/licenses/by-nc/4.0/>).

crust. Fluids at studied P - T conditions play a decisive role in the formation of hydrothermal ore deposits, including most of the world's gold deposits.

Keywords: High Pressure; Elevated Temperature; Equation of State; Water-Carbon Dioxide Fluid; Phase Splitting; Upper Crust; NaCl; CaCl₂

1. Introduction

Fluids of the earth's crust play an extremely important role in all geological processes of formation and transformation of the earth's crust—magmatism, metamorphism, metasomatism, petrogenesis, and geodynamics. Dissolving, transportation, and deposition of substances by aqueous fluids of the upper crust are the principal processes responsible for the formation of hydrothermal ore deposits of metals, including the most deposits of gold on Earth^[1–3]. The physicochemical properties of fluids vary greatly as they depend on the P - T parameters and compositions of fluids in different geological settings, and these differences strongly influence petrogenesis processes at different depth levels. Such properties include, in particular, the phase state of fluids (homogeneous or heterogeneous), the chemical composition and density of fluid phases, which affect their dissolving capacity, and activities of the components of the fluid. NaCl and CO₂ are very common components of the aqueous fluids, both in the lower and middle crust at supercritical P - T conditions and in the upper crust at subcritical P - T . In both cases, the presence of CO₂ leads to the possibility of splitting the fluid into coexisting fluid phases. At subcritical P - T conditions, this is the splitting of the CO₂-containing fluids at pressures above saturated vapor pressure. For the P - T conditions of the upper crust, thermodynamic models of the fluid system H₂O-CO₂-NaCl were developed in the works^[4–13]. Most of the fluid models are limited by low and moderate concentrations of salt. In particular, this is due to the use of the Pitzer model, which is limited in molality of NaCl by $m_{\text{NaCl}} \leq 6$ ^[14–16].

Along with NaCl, CaCl₂ is a common component of natural aqueous fluids. Despite this fact, the system H₂O-CO₂-CaCl₂ is much less studied theoretically. There are experimental studies of the system at supercritical P - T conditions^[17–19]. Based on these experimental results, an equation of state for this system at supercritical P - T conditions was proposed in the work^[20]. One of the goals of the present work is the development of a thermodynamic model for the

ternary system H₂O-CO₂-CaCl₂ for the subcritical P - T region. The mixtures of NaCl and CaCl₂ are encountered quite often in the core fluids^[21]. A thermodynamic model for the quaternary fluid system H₂O-CO₂-NaCl-CaCl₂ for the supercritical P - T conditions was proposed in the work^[22]. It was shown that the properties of the system with the mixed salt composition can be qualitatively different from their edge ternary systems with one salt. The salt compositions of NaCl-CaCl₂ mixed fluids are correlated^[21] with their total salinities and the depths they are located. Larger salinities and depths are associated with larger CaCl₂ content, whereas less saline and nearer to the surface fluids demonstrate a prevalence of NaCl in salt. A possible explanation of this fact was proposed in the work^[23].

At supercritical conditions, H₂O and CO₂ can be mixed in any proportions. A homogeneous fluid can split into coexisting fluid phases only due to different affinities of salts to H₂O and CO₂. In many cases, the properties of the two coexisting phases do not demonstrate sharp differences. This means that the thermodynamics of both phases can be described by the same equations. This approach was applied in works^[20,22,24,25]. The situation in the subcritical region is different. In a wide P - T region, the miscibility of H₂O and CO₂ is limited. In this region, the two possibly coexisting phases are sharply different in properties. The liquid phase consists of water with salts and some portion of dissolved CO₂. The gas phase contains a prevalent portion of CO₂. The water vapor contained in the gas phase has a low density and does not have the properties of liquid water, such as the possibility to dissolve large amounts of salts. These features of the subcritical region are taken into account in the models developed below. The thermodynamic models presented below are free from the limitation with respect to the mole fractions of the salts, because they are based on the models^[16,26] of brines H₂O-NaCl and H₂O-CaCl₂, valid from dilute solutions up to the limit of solubility of the corresponding salt. The goals of the present work are development for the subcritical P - T region: 1. New thermo-

dynamic models of the ternary systems $\text{H}_2\text{O}-\text{NaCl}-\text{CaCl}_2$ and $\text{H}_2\text{O}-\text{CO}_2-\text{NaCl}$ applicable for arbitrary mole fractions of the salts; 2. Thermodynamic model of the ternary system $\text{H}_2\text{O}-\text{CO}_2-\text{CaCl}_2$ also applicable for the arbitrary mole fraction of CaCl_2 ; 3. the thermodynamic model for the quaternary fluid system $\text{H}_2\text{O}-\text{CO}_2-\text{NaCl}-\text{CaCl}_2$.

2. Methods

Our equation of state (EOS) is formulated in terms of the Gibbs free energy. The equation for the Gibbs free energy of mixing G^{mix} is a sum of the entropy term and energy terms for interactions between the components of the system. It looks like

$$G^{\text{mix}} = -TS + G_{134} + G_{12} + G_{23} + G_{24} \quad (1)$$

Here S is the entropy, and T is the temperature in Kelvin. The terms G with subscripts relate to the energy of the interaction between the corresponding components. Here and in the following 1 stays for H_2O , 2 for CO_2 , 3 for NaCl , and 4 for CaCl_2 .

2.1. Entropy of Mixing

In the absence of the dissociation of the components, the entropy of mixing of four components for one mol of the mixture would look like

$$S = -R(x_1 \ln x_1 + x_2 \ln x_2 + x_3 \ln x_3 + x_4 \ln x_4) \quad (2)$$

where x_i are the mole fractions of components, $x_i = N_i/N$,

N_i is the number the molecules of kind i in the system, $N = \sum_i N_i$ is the total number of molecules in the system. R is the universal gas constant. The formula for the case of a partial dissociation of NaCl and CaCl_2 can be derived analogously to Equation (2) from the fundamental equation

$$S = k \ln W \quad (3)$$

where k is the Boltzmann constant, and W is the number of different ways, in which the particles in the system can be arranged with the same total energy of the system^[27]. The values W are also considered as weights of configurations with certain fixed energies in the partition function^[27]. Direct using the full partition functions is convenient in *ab initio* calculations or calculations formally near to *ab initio*^[28–32]. The energy terms in the model presented in this paper are empirical. Thus, we do not construct the partition function, but consider the entropy and energy terms separately.

We retain the notation N_3 for the stoichiometric number of molecules NaCl , i.e., for the sum of NaCl molecules and Na^+Cl^- pairs. Analogously, N_4 is the stoichiometric number of molecules CaCl_2 . When α_3 is the degree of dissociation of NaCl , the system contains $\alpha_3 N_3$ ions Na^+ and the same number of ions Cl^- . Additionally, there are $(1-\alpha_3)N_3$ non-dissociated molecules NaCl . Analogously, dissolution of CaCl_2 results in emerging of $\alpha_4 N_4$ ions Ca^{2+} and $2\alpha_4 N_4$ ions Cl^- . The total number of the Cl^- ions is $\alpha_3 N_3 + 2\alpha_4 N_4$. The system also contains $(1-\alpha_4)N_4$ non-dissociated molecules CaCl_2 . The total number of particles in the system is $N_1 + N_2 + (1 + \alpha_3) N_3 + (1 + 2\alpha_4) N_4$. The number of the energetically equivalent combinations is

$$W = \frac{[N_1 + N_2 + (1 + \alpha_3) N_3 + (1 + 2\alpha_4) N_4]!}{N_1! N_2! (\alpha_3 N_3)! [(1 - \alpha_3) N_3]! (\alpha_4 N_4)! [(1 - \alpha_4) N_4]! (\alpha_3 N_3 + 2\alpha_4 N_4)!} \quad (4)$$

It follows from Equations (3) and (4) that

$$\begin{aligned} S = -kN \{ & x_1 \ln x_1 + x_2 \ln x_2 \\ & + (1 - \alpha_3) x_3 \ln [(1 - \alpha_3) x_3] \\ & + (1 - \alpha_4) x_4 \ln [(1 - \alpha_4) x_4] \\ & + \alpha_3 x_3 \ln(\alpha_3 x_3) + \alpha_4 x_4 \ln(\alpha_4 x_4) \\ & + (\alpha_3 x_3 + 2\alpha_4 x_4) \ln(\alpha_3 x_3 + 2\alpha_4 x_4) \\ & - (1 + \alpha_3 x_3 + 2\alpha_4 x_4) \ln(1 + \alpha_3 x_3 + 2\alpha_4 x_4) \} \end{aligned} \quad (5)$$

When $\alpha_3 = \alpha_4 = 1$, which is assumed in the models^[16,26] of $\text{H}_2\text{O}-\text{NaCl}$ and $\text{H}_2\text{O}-\text{CaCl}_2$ systems, the entropy term in G^{mix} per one (stoichiometric) mol of the fluid $\text{H}_2\text{O}-\text{CO}_2-\text{NaCl}-\text{CaCl}_2$ is

$$\begin{aligned} -TS = RT \{ & x_1 \ln x_1 + x_2 \ln x_2 + x_3 \ln x_3 \\ & + x_4 \ln x_4 + (x_3 + 2x_4) \ln(x_3 + 2x_4) \\ & - (1 + x_3 + 2x_4) \ln(1 + x_3 + 2x_4) \} \end{aligned} \quad (6)$$

2.2. System H₂O-NaCl-CaCl₂

Thermodynamic models of the brines H₂O-NaCl and H₂O-CaCl₂ obtained in works^[16,26] can precisely reproduce the behavior of these systems from the minimal mole fractions of salts (where the main effects are due the long-range electrostatic interaction and its screening) up to the high mole fractions corresponding to the limit of solubility of the salts. The model for H₂O-NaCl is valid for temperatures ranging from 150 °C to 300 °C and pressures up to 5 kbar. The model for H₂O-CaCl₂ is valid for temperatures 150–350 °C and pressures up to 0.7 kbar. In the current work, we use energy terms for the subsystems H₂O-NaCl and H₂O-CaCl₂ as they were obtained in the thermodynamic models^[16,26]. The entropy terms in the Gibbs free energy of mixing employed in models^[16,26] are different from that given by Equation (6) at $x_2 = x_4 = 0$ and $x_2 = x_3 = 0$ correspondingly. Nevertheless, these models can be used with the entropy term (6) with their energy terms and corresponding numerical parameters. Indeed, the entropy-dependent parts of the chemical potential of water μ_{1s} given by equations of Ivanov et al.^[16] and Ivanov et al.^[26] coincide with that following from (6),

$$\mu_{1s} = RT \{ \ln x_1 - \ln (1 + x_3 + 2x_4) \}$$

at $x_4=0$ for H₂O-NaCl and at $x_3=0$ for H₂O-CaCl₂. The parameters of the models at the vapor-saturated pressure^[16] were obtained by fitting experimental data on the osmotic coefficient ϕ which depends only on the chemical potential of water μ_1 . The pressure dependences obtained in^[26] can also be retained due to independence of the entropy terms both of^[16,26] and (6) on the pressure.

He thermodynamic behavior of the ternary system with two salts, H₂O-NaCl-CaCl₂, can depend not only on the properties of the binary subsystems, H₂O-NaCl and H₂O-CaCl₂, and their statistical interaction through the entropy of the mixing, but also it can depend on possible interaction energy between dissolved NaCl and CaCl₂. A term of this kind, i.e., $W_{34}x_3x_4$ was included to the G^{mix} for the system H₂O-CO₂-NaCl-CaCl₂ at supercritical P - T conditions in^[22]. Due to the lack of experimental data on the water-containing systems, it was obtained in the form of a constant number $W_{34} = -10.3$ kJ/mol from the experimental data on the liquidus in the NaCl-CaCl₂ system. On the other hand, for the lower P - T conditions, which we consider here, there

are experimental data^[33] on $PVTx$ properties of the system H₂O-NaCl-CaCl₂. In this work, the densities of the system H₂O-NaCl-CaCl₂ were obtained for temperatures from 298.15 K to 523.15 K.

Models^[16,26] of H₂O-NaCl and H₂O-CaCl₂ are obtained for temperatures 423.15 K and above, so we fit our parameter of the interaction between NaCl and CaCl₂ in the aquatic environment on two series of measures presented in^[33], namely 473.15 K and 523.15 K. Pressures in these experimental series vary from 2 MPa to 70 MPa, the molality of the brines are between 0.01 mol/kg and 6 mol/kg (for NaCl). The latter value of the salt concentration is much lower than the saturation concentrations of the solutions, which are the upper limits for models of^[16,26], but the data^[33] are satisfactory for obtaining a simple form of the parameterization of the interaction between NaCl and CaCl₂ presented below.

The density of the system, described by its Gibbs free energy can be obtained from the mole volume V of the system. The latter can be calculated by the equation

$$V = \left(\frac{\partial G}{\partial P} \right)_{T, x_i} \quad (7)$$

where G is the total Gibbs free energy of the system, which includes the Gibbs energies of the components G_i and G^{mix} . For the mole volume this gives

$$V = \sum_{i=1}^4 V_i x_i + \left(\frac{\partial G^{\text{mix}}}{\partial P} \right)_{T, x_i} \quad (8)$$

where V_i are the mole volumes of the components. For V_1 and V_2 we use values given by thermodynamic models IAPWS95 for water^[34] and a similar model^[35] for CO₂. For V_3 and V_4 we use values belonging to the models^[26]. The excess volume due to mixing of components is given by the last term in the Equation (8). For the subsystem H₂O-NaCl-CaCl₂ this is effect of mixing the salts in the brine.

The term $W_{34}x_3x_4$ with a constant value used in^[22] does not affect the value of V due to its derivative with respect to P is equal to zero. Thus, the reproduction of the experimental data on the density of the H₂O-NaCl-CaCl₂ fluid containing both NaCl and CaCl₂ requires introducing additional terms into G^{mix} , dependent on the pressure. For this purpose, the term

$$G_{34p} = (W_{34p1}/V_1^3) x_3x_4 \quad (9)$$

was added to G^{mix} . The value of the numerical parameter $W_{34\text{p1}}$ was obtained by fitting on the results of^[33] for $\text{H}_2\text{O}-\text{NaCl}-\text{CaCl}_2$ which include 287 data points for temperatures 523 K and 473 K. The result of fitting is the value of $W_{34\text{p1}} = 7.9336416 \cdot 10^6 \text{ J/mol} \cdot (\text{cm}^3/\text{mol})^3$. The differences in the fluid densities between values given by Equation (9) ρ_8 and experimental data^[33] ρ_{exp} , i.e., $\Delta\rho = \rho_8 - \rho_{\text{exp}}$ are presented in **Figure 1** as dependent on the molality of CaCl_2 m_4 related to the sum of molalities of both CaCl_2 and NaCl (m_3). The maximal molality of the CaCl_2 in the experimental

data^[33] was $m_4 = 3 \text{ mol/kg}$, whereas the error of this value was evaluated by the authors as $\sigma m_4 = 0.064 \text{ mol/kg}$. Thus, the relative error of the m_4 was about 2%. The maximal deviation of the density of the brine from the density of the pure water was about 0.3 g/cm^3 . Thus, the error in the experimental densities of brines can be evaluated as $\sigma\rho = 6 \cdot 10^{-3} \text{ g/cm}^3$. Strictly speaking, all the $\Delta\rho$ values, presented in **Figure 1** correspond to this estimation. But several most deviating points (squares in **Figure 1**) were excluded from the final fit of $W_{34\text{p1}}$.

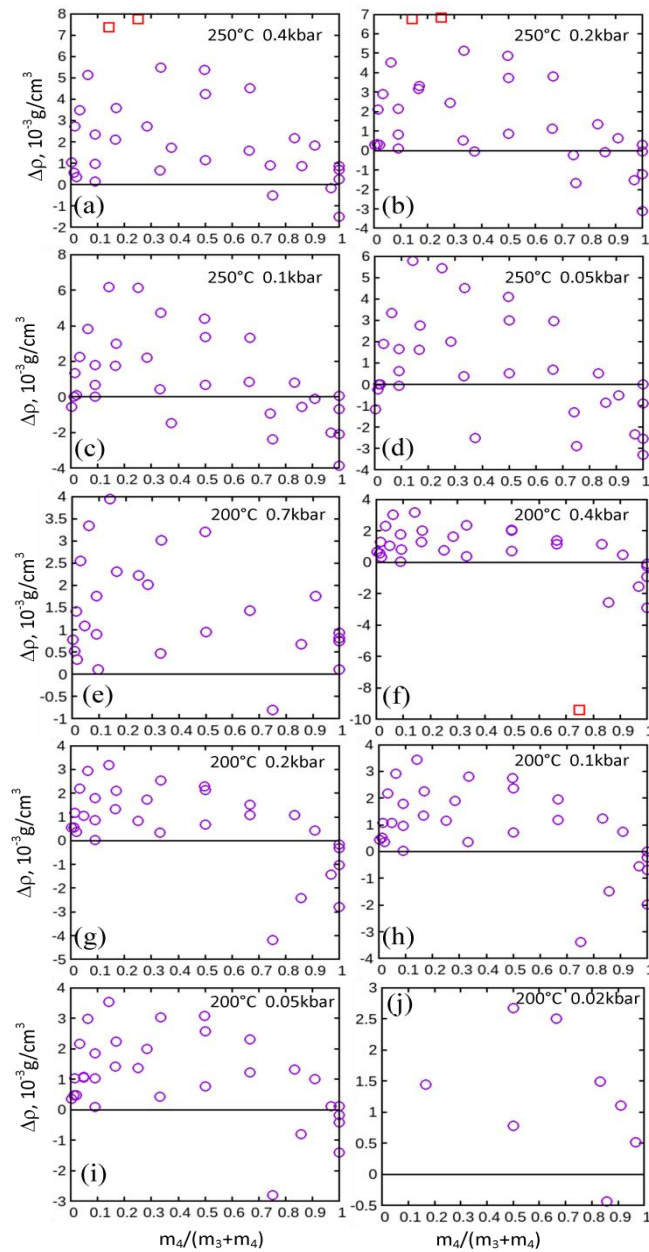


Figure 1. Differences between experimental data^[33] and our approximation via Equation (9). Circles are points used for fitting $W_{34\text{p1}}$. Squares are points excluded from the fit.

The value of G_{34p} decreases with decreasing the density of water. The value of W_{34} was obtained in^[22] for a water-free system, and it is reasonable to retain the corresponding term for the limit of the infinite V_1 . Thus, finally, the term for the interaction of NaCl and CaCl_2 looks like

$$G_{34} = W_{34a}x_3x_4 = (W_{34} + W_{34p1}/V_1^3) x_3x_4 \quad (10)$$

For the ternary system H_2O -NaCl- CaCl_2 the energy term in the G^{mix} is

$$G_{134} = G_{13} + G_{14} + G_{34} \quad (11)$$

where terms G_{13} and G_{14} for interactions H_2O -NaCl and H_2O - CaCl_2 are obtained in the works^[16,26].

2.3. System H_2O - CO_2

The excess Gibbs free energy of mixing for the system H_2O - CO_2 at temperatures 50–350 °C and pressures 0.2–3.5 kbar was obtained in^[36] based on the experimental results of the work^[37]. The term for the interaction energy between H_2O and CO_2 molecules has a form of the Van Laar equation with parameters A_{12} and A_{21} fitted on experimental data. For systems that include components additional to H_2O and CO_2 , this term G_{12} is to be modified by introducing a multiplier (x_1+x_2) . As result, it has a form

$$G_{12} = RT \frac{A_{12}x_1A_{21}x_2}{A_{12}x_1+A_{21}x_2} (x_1 + x_2) \quad (12)$$

Mole volumes of H_2O and CO_2 containing in the equations for A_{12} and A_{21} are expressed via equations of state IAPWS95^[34] for water and^[35] for CO_2 . The same equations of state^[34,35] were applied below for calculations of the total G and its derivatives for the fluid phases.

2.4. Systems H_2O - CO_2 -NaCl and H_2O - CO_2 - CaCl_2

2.4.1. Gas Phase

The density of NaCl in the water vapor was studied in experimental and theoretical works^[38–40]. At relatively low temperatures, we consider in this paper, the concentrations of NaCl in H_2O - CO_2 gas phase are very low. In particular, this fact can justify the assumption of zero concentration of NaCl in the gas phase made in the works^[10,11]. However,

opposite to these works, we base our thermodynamic model on equations for the Gibbs free energy. This means that the low mole fraction of NaCl in the gas phase should follow from the form of the equation for G^{mix} .

The density of the water vapor in the gas phase is too low to induce dissociation of molecules of NaCl. Both the absence of NaCl dissociation and low densities of H_2O and CO_2 in the gas phase justify the assumption that NaCl is present in this phase as a vapor of NaCl molecules. We neglect a possible interaction of the NaCl molecules with molecules of H_2O and CO_2 . For a rough evaluation of the concentration of NaCl in the gas phase, it was assumed that the transition of NaCl molecules from the liquid to the gas phase can be associated with the Gibbs free energy of vaporization of NaCl, i.e., $\Delta G_{\text{NaCl_gas}} = \Delta G_{\text{NaCl_vapor}} \approx 180 \text{ kJ/mol}$ ^[41]. Our test calculations show that decreasing $\Delta G_{\text{NaCl_gas}}$ to $\Delta G_{\text{NaCl_gas}} = 50 \text{ kJ/mol}$ leads to increasing the mole fraction of NaCl in the gas phase, e.g., from $x_{\text{NaCl,g}} = 0.2 \cdot 10^{-4}$ to $x_{\text{NaCl,g}} = 1.0 \cdot 10^{-4}$ with a negligibly small effect on other parameters of coexisting gas and liquid phases and position of the solvus. Increasing the value of $\Delta G_{\text{NaCl_gas}}$ above $\Delta G_{\text{NaCl_gas}} = 180 \text{ kJ/mol}$ results in even smaller effects. This means that the value of the Gibbs free energy of solvation, which is about 4 kJ/mol, and the temperature dependence of $\Delta G_{\text{NaCl_vapor}}$ practically have no effect on the critical behavior of the fluid system H_2O - CO_2 -NaCl.

The maximal mole fraction of NaCl in the gas phase in calculations with $\Delta G_{\text{NaCl_gas}} = 180 \text{ kJ/mol}$ is about $x_{\text{NaCl}} = 3 \cdot 10^{-5}$. For example, this value was achieved in calculations for H_2O - CO_2 -NaCl at the temperature 350 °C and pressure 0.3 kbar. This value can be compared with the experimental result of the work^[38]. The authors of this work obtained the saturated $x_{\text{NaCl}} = 0.8 \cdot 10^{-5}$ in water vapor at 350 °C and 0.114 kbar. Taking into account a decrease of the saturate concentration of gaseous NaCl with decreasing pressure, our value of x_{NaCl} can be considered to be in agreement with that experimental value. The experimental results^[38] relate to the NaCl in the water vapor. The mole fraction of NaCl in pure CO_2 atmosphere is even lower than in H_2O vapor. Experiments^[42] on this system give $x_{\text{NaCl}} = 1.36 \cdot 10^{-6}$ for 300 °C and 0.65 kbar, and $x_{\text{NaCl}} = 0.16 \cdot 10^{-6}$ for 300 °C and 0.33 kbar.

The argumentation on the simulation of the gas phase of H_2O - CO_2 -NaCl, presented above, is also valid for the

system $\text{H}_2\text{O}-\text{CO}_2-\text{CaCl}_2$. For CaCl_2 in the $\text{H}_2\text{O}-\text{CO}_2$ gas phase we used $\Delta G_{\text{CaCl}_2, \text{gas}} = 250 \text{ kJ/mol}$ which is near to its Gibbs free energy of vaporization^[41].

Thus, the energy terms for the gas phase can be written as

$$G_{13g} = \Delta G_{\text{NaCl}_{\text{gas}}x_3}; \quad G_{23g} = 0 \quad (13)$$

and

$$G_{14g} = \Delta G_{\text{CaCl}_2, \text{gas}}x_4; \quad G_{24g} = 0 \quad (14)$$

Such a form of the x_{NaCl} and x_{CaCl_2} dependent terms of the Gibbs free energy in the gas phase provides small and near in the order of magnitude to the experimental values of the mole fractions of the salts. The entropy for the gas phase has a form (2) due to $\alpha_3 = \alpha_4 = 0$ in the gas phase.

2.4.2. Liquid Phase

In addition to the energy terms G_{12} , G_{13} , and G_{14} , the thermodynamic description of the ternary systems $\text{H}_2\text{O}-\text{CO}_2-\text{NaCl}$ and $\text{H}_2\text{O}-\text{CO}_2-\text{CaCl}_2$ requires terms G_{23} and G_{24} in the liquid phase, for $\text{H}_2\text{O}-\text{CO}_2-\text{NaCl}$ and $\text{H}_2\text{O}-\text{CO}_2-\text{CaCl}_2$, respectively. We start with the system $\text{H}_2\text{O}-\text{CO}_2-\text{NaCl}$. For this system, there are experimental data obtained during several decades. The most convenient for our aims are data of the work^[43]. This work contains a large set of compositions (x_1 , x_2 , x_3) of the liquid water-salt phase (also containing CO_2) coexisting in equilibrium with gaseous CO_2 -water vapor phase. Thus, these experimental data are compositions of the system on the solvus. For three temperatures, 150 °C, 250 °C, and 350 °C, the compositions of the liquid phase are presented for two different mole fractions of NaCl at the same P and T . This simplifies fitting the experimental data with functions containing two fitting parameters. We have

$$\begin{aligned} a_{21} &= 77624; \quad a_{22} = 73.051; \quad a_{23} = 1.2634; \quad a_{24} = 8443.8; \quad a_{25} = 1.6595; \quad a_{26} = 205.12; \\ a_{31} &= -3.4288; \quad a_{32} = -246.95; \quad a_{33} = -25825; \quad a_{34} = 77767. \end{aligned}$$

The solvuses obtained from G^{mix} using the Equation (16) are presented in **Figure 2** by bold green curves. It is seen that this approximation is in a good agreement with both the experimental points used in obtaining of this approximation (**Figures 2a, 2b, 2e, 2f, and 2h**) and with points which were not involved in obtaining Equation (16) (**Figures 2c, 2d, and**

taken the term G_{23} responsible for the interaction of NaCl with CO_2 in the liquid phase in the form

$$G_{23} = x_2x_3 \frac{W_{23}x_2 + W_{32}x_3}{x_2 + x_3} \quad (15)$$

with parameters W_{23} and W_{32} . This form of the G_{23} coincides with that used in thermodynamic models^[24,25] of the ternary system $\text{H}_2\text{O}-\text{CO}_2-\text{NaCl}$ at supercritical P - T conditions, as well as in the model^[22] of quaternary system $\text{H}_2\text{O}-\text{CO}_2-\text{NaCl}-\text{CaCl}_2$ at supercritical P - T conditions. Equation (15) together with the assumptions made with respect to the thermodynamics of the gas phase expressed in Equation (13) allows obtaining a complete form of the G^{mix} for the system $\text{H}_2\text{O}-\text{CO}_2-\text{NaCl}$ and defines the phase state (homogeneous or two-phase) of the system at given temperatures, pressures, values of W_{23} and W_{32} , and compositions of the system.

The values of W_{23} and W_{32} were obtained for all 22 P - T points of the work^[43] containing pairs of the compositions of the liquid phase being in equilibrium with the gas phase. The knowledge of these values makes it possible to build solvuses for the corresponding P and T . Examples of such solvuses are presented in **Figures 2a, 2b, 2e, 2f, and 2h** by broken lines. The availability of arrays of W_{23} and W_{32} values for a number of different P and T makes it possible to obtain approximate dependences of these two parameters on P and T . The arrays of W_{23} and W_{32} obtained for discrete sets of P and T can be approximated with formulas

$$\begin{aligned} W_{23} &= a_{21} + a_{23}(t - a_{22})^2 - \frac{a_{24} + a_{25}(t - a_{26})^2}{P} \\ W_{32} &= a_{31}(t - a_{32})^2 + a_{33}P + a_{34} \end{aligned} \quad (16)$$

where t is the temperature in °C and P is the pressure in kbar. The values of the parameters in Equation (16) are

2g).

For the interaction of CaCl_2 with CO_2 in the liquid phase of the fluid $\text{H}_2\text{O}-\text{CO}_2-\text{CaCl}_2$, we used the form analogous to Equation (15), *i.e.*,

$$G_{24} = x_2x_4 \frac{W_{24}x_2 + W_{42}x_4}{x_2 + x_4} \quad (17)$$

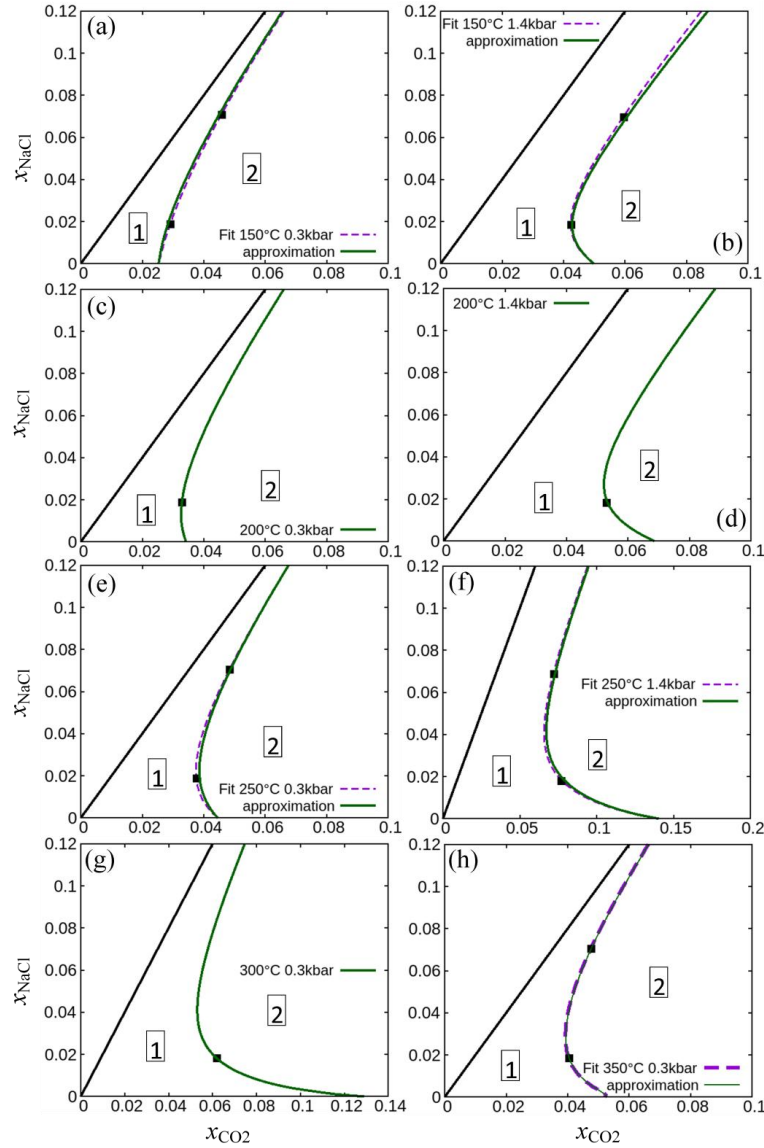


Figure 2. Phase diagrams of the system $\text{H}_2\text{O}-\text{CO}_2-\text{NaCl}$. Filled squares are experimental points of the work^[43]. Broken lines are solvuses obtained by fitting W_{23} and W_{32} on pairs experimental points for one P - T combination. Solid green curves are solvuses according Equation (16). Numbers in frames denote areas (fields) of different phase composition: (1) homogeneous fluid (liquid phase); and (2) two coexisting (liquid and gas) phases.

For every P - T point, the experimental data of the works^[44,45] for the fluid $\text{H}_2\text{O}-\text{CO}_2-\text{CaCl}_2$ contain only one composition of the liquid phase being in an equilibrium with the gas phase. This makes impossible to obtain two parameters, W_{24} and W_{42} for separated P - T points. For these parameters we assumed that they differ from W_{23} and W_{32} by a multiplier $q(P, T)$, the same for both W_{24} and W_{42} :

$$\begin{aligned} W_{24}(P, t) &= q(P, t)W_{23}(P, t) \\ W_{42}(P, t) &= q(P, t)W_{32}(P, t) \end{aligned} \quad (18)$$

Fitting the experimental data^[44] gives the following

approximation for $q(P, t)$:

$$q = b_2 (P - b_0) (t - b_1)^3 + b_3 \quad (19)$$

where

$$\begin{aligned} b_0 &= 0.39614; \quad b_1 = 106.27; \\ b_2 &= -7.4634 \times 10^{-7}; \quad b_3 = 1.3765 \end{aligned} \quad (20)$$

Several examples of solvuses in the system $\text{H}_2\text{O}-\text{CO}_2-\text{CaCl}_2$ obtained with Equations (18) and (19) are given in **Figures 3a, 3e, 3i, and 3m**. **Figures 3a, 3e, and 3i** show a full agreement of the approximation Equations (18) and (19) with the experimental data.

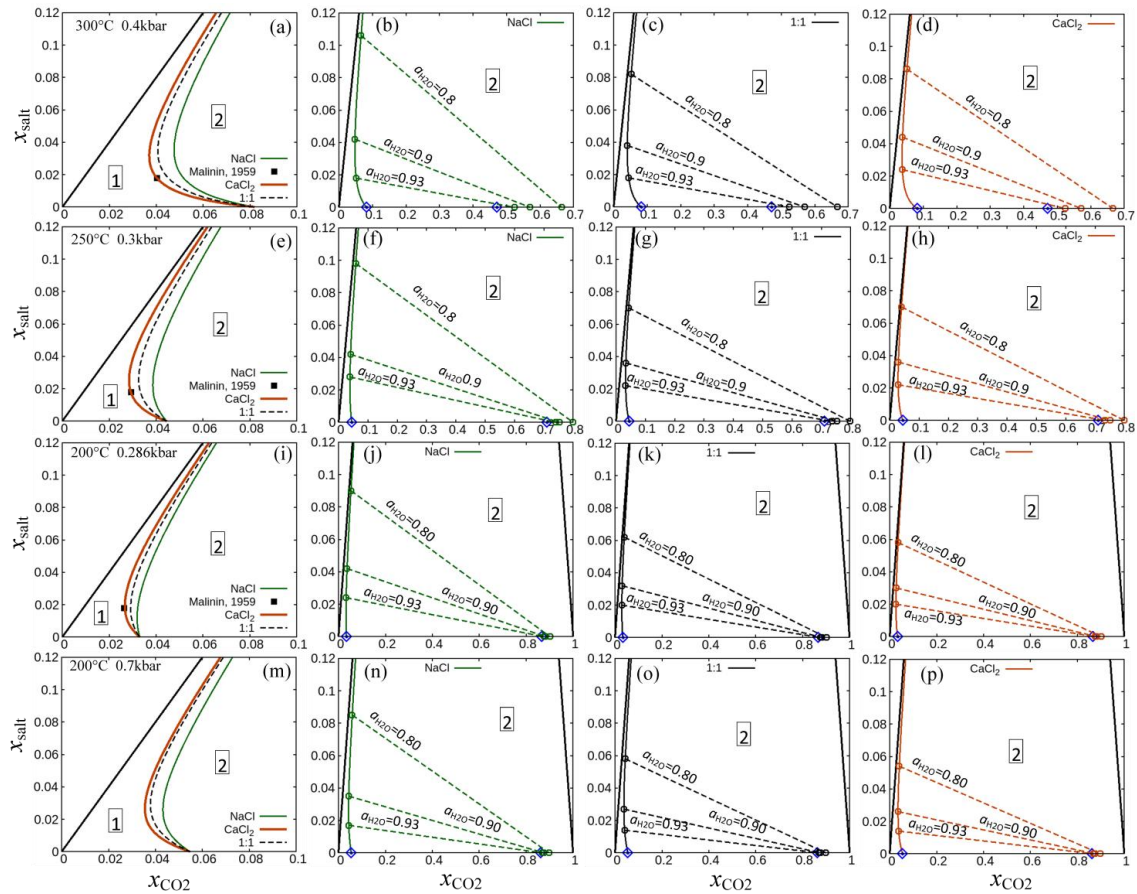


Figure 3. Phase diagrams for ternary $\text{H}_2\text{O}-\text{CO}_2-\text{NaCl}$ and $\text{H}_2\text{O}-\text{CO}_2-\text{CaCl}_2$, and quaternary $\text{H}_2\text{O}-\text{CO}_2-\text{NaCl}-\text{CaCl}_2$ fluids. Panels a, e, i, m—solvuses for $\text{H}_2\text{O}-\text{CO}_2-\text{CaCl}_2$ and for $\text{H}_2\text{O}-\text{CO}_2-\text{NaCl}-\text{CaCl}_2$ when $x_{\text{NaCl}}:x_{\text{CaCl}_2} = 1:1$ compared with solvuses for $\text{H}_2\text{O}-\text{CO}_2-\text{NaCl}$. Filled squares are experimental points^[44] for $\text{H}_2\text{O}-\text{CO}_2-\text{CaCl}_2$. Other panels are solvuses (bold curves) and tie lines (dotted straight lines) for $\text{H}_2\text{O}-\text{CO}_2-\text{NaCl}$ (b, f, j, n), $\text{H}_2\text{O}-\text{CO}_2$ -salt at $x_{\text{NaCl}}/x_{\text{salt}} = 0.5$ (c, g, k, o), and $\text{H}_2\text{O}-\text{CO}_2-\text{CaCl}_2$ (d, h, l, p). Blue diamonds are the boundaries of the gap in the miscibility of H_2O and CO_2 . Numbers in frames denote areas (fields) of different phase composition: (1) homogeneous fluid (liquid phase); and (2) two coexisting (liquid and gas) phases.

A comparison of the solvuses for $\text{H}_2\text{O}-\text{CO}_2-\text{NaCl}$ and $\text{H}_2\text{O}-\text{CO}_2-\text{CaCl}_2$ shows a smaller size of the field of the homogeneous fluid for $\text{H}_2\text{O}-\text{CO}_2-\text{CaCl}_2$ compared to $\text{H}_2\text{O}-\text{CO}_2-\text{NaCl}$. This indicates a greater affinity of CO_2 for NaCl in the subcritical aqueous fluids compared to the affinity of CO_2 for CaCl_2 . For supercritical fluids, this feature was demonstrated in the work^[23]. Now, it is possible to conclude that this difference in the affinity of CO_2 for NaCl and CaCl_2 is a general property of the aqueous fluids, independent on their P - T regime, both sub- and supercritical.

3. Results and Discussion

In the previous section, we have obtained all the terms present in the Gibbs free energy of mixing (1) for the quaternary system $\text{H}_2\text{O}-\text{CO}_2-\text{NaCl}-\text{CaCl}_2$. This finalizes the build-

ing of the numerical thermodynamic model of this system and opens a possibility to study the properties both ternary systems with one salt in the fluid and the quaternary system with a mixed salt composition. **Figures 3a, 3e, 3i, and 3m** contain both phase diagrams of ternary systems $\text{H}_2\text{O}-\text{CO}_2-\text{NaCl}$ and $\text{H}_2\text{O}-\text{CO}_2-\text{CaCl}_2$, and also phase diagrams of a quasi-ternary system $\text{H}_2\text{O}-\text{CO}_2$ -salt with $x_{\text{salt}} = x_{\text{NaCl}} + x_{\text{CaCl}_2}$ and a fixed ratio $x_{\text{NaCl}}/x_{\text{salt}} = 0.5$. The other panels of **Figure 3** are phase diagrams for all three cases: $x_{\text{NaCl}}/x_{\text{salt}} = 1$, $x_{\text{NaCl}}/x_{\text{salt}} = 0.5$, and $x_{\text{NaCl}}/x_{\text{salt}} = 0$ with the tie lines connecting the points and corresponding compositions of coexisting liquid and gas phases. For the ternary systems like $\text{H}_2\text{O}-\text{CO}_2-\text{NaCl}$ and $\text{H}_2\text{O}-\text{CO}_2-\text{CaCl}_2$ with one salt, the tie lines are to be straight lines with constant compositions of the coexisting phases along these lines. The activities of the components are also to be constant on the tie lines. It was

found^[22] that in the quaternary fluid system $\text{H}_2\text{O}-\text{CO}_2-\text{NaCl}-\text{CaCl}_2$ at supercritical P - T conditions, the lines of constant activities of components are not straight lines in the field of two coexisting fluids due to the redistribution of salts between two fluid phases. This effect does not present at the subcritical conditions we consider in this paper due to negligibly small concentrations of salts in the gas phase. Thus, the tie lines for the systems $\text{H}_2\text{O}-\text{CO}_2$ -salt at constant $x_{\text{NaCl}}/x_{\text{salt}}$ ($x_{\text{NaCl}}/x_{\text{salt}} = 0.5$ in **Figures 3c, 3g, 3k, 3o**) are also straight lines with constant compositions of the coexisting phases and constant activities of components on them.

A specific feature of these tie lines is that they connect two separate regions. In the supercritical P - T region, the tie lines connect pairs of points lying on one continuous solvus with a critical point separating the parts of the solvus corresponding to different phases of the fluid. Opposite to this picture, the right ends of the tie lines in **Figure 3** do not belong to the solvus lines on the left side of the phase diagram, but lie very near to the horizontal axis (the distance is not visible in the scale of the picture). In fact, there is a second solvus, lying on the right near to the horizontal axis and separated from the left one by the gap in the solubility of CO_2 in pure water. An important feature of the mutual behavior of the liquid and gas phases is that the increase of the mole fraction of the salt in the liquid phase results in a

decrease in the mole fraction of water in the gas phase. This shifts the composition of the gas phase towards to the pure CO_2 .

The equations for chemical potentials and activities of components obtained from (1) are given in the Supplementary Material. The equations for activities of H_2O and CO_2 are valid for all the compositions of the quaternary system $\text{H}_2\text{O}-\text{CO}_2-\text{NaCl}-\text{CaCl}_2$. Activities of NaCl and CaCl_2 can be calculated only for corresponding ternary systems with one salt, because these salts do not exist as separate compounds in aqueous fluids with two salts.

One can see in **Figure 3** that the compositions of the liquid phase corresponding to the same activity of water $a_{\text{H}_2\text{O}}$ depend rather strongly on the ratio of mole fractions of NaCl and CaCl_2 . Such type of dependence exists also in solutions with no CO_2 . In **Figure 4**, we demonstrate the effect in the aqueous system. In **Figure 4a**, the activity of water is shown as a function of the mole fraction of the salt for various portions of CaCl_2 in the total composition of the salt. It is observed that the activity of water have the largest values for the pure NaCl as a salt. The addition of CaCl_2 leads to a strong decrease of $a_{\text{H}_2\text{O}}$. However, this effect tends to a saturation at $x_{\text{CaCl}_2}/x_{\text{salt}} \geq 0.5$. The dependence of $a_{\text{H}_2\text{O}}$ on $x_{\text{CaCl}_2}/x_{\text{salt}}$ at a constant $x_{\text{salt}} = 0.1$ is presented in **Figure 4b**.

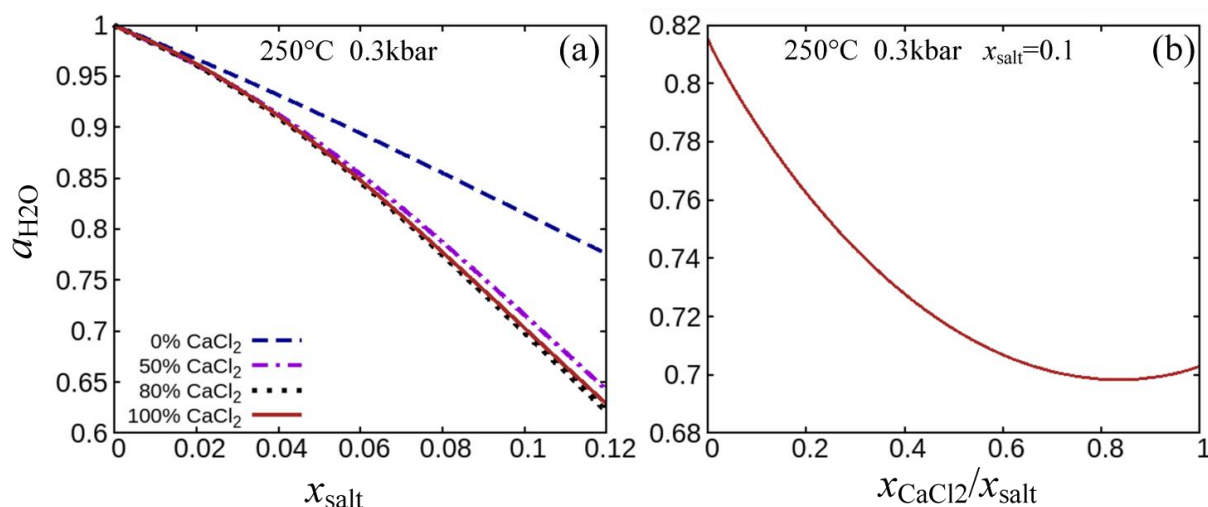


Figure 4. Activity of water: (a) $a_{\text{H}_2\text{O}}$ dependent on the salt mole fractions for different proportions of NaCl and CaCl_2 ; and (b) $a_{\text{H}_2\text{O}}$ dependent on the portion of CaCl_2 in the salt at the constant total salt fraction $x_{\text{salt}} = x_{\text{NaCl}} + x_{\text{CaCl}_2} = 0.1$.

The densities of fluid phases emerging in result of the splitting of a homogeneous fluid into two coexisting phases play an important role in the following spatial separation of

these phases. In **Figures 5, 6, and 7**, we show densities of both liquid and gas phases as functions of the x_{salt} (along the solvus) for three compositions of the salt in the fluid. **Figure**

5 is for pure NaCl, **Figure 6** is for pure CaCl_2 , and **Figure 7** is for $x_{\text{NaCl}} = x_{\text{CaCl}_2}$. In some cases, the density of the gas phase can reach rather big values due a high pressure and a prevalent portion of CO_2 having a large molecular mass

compared to water. Nevertheless, in all the cases, the density of the liquid phase is larger than the density of the gas phase. The density of the liquid phase increases with the growth of the salt content in it.

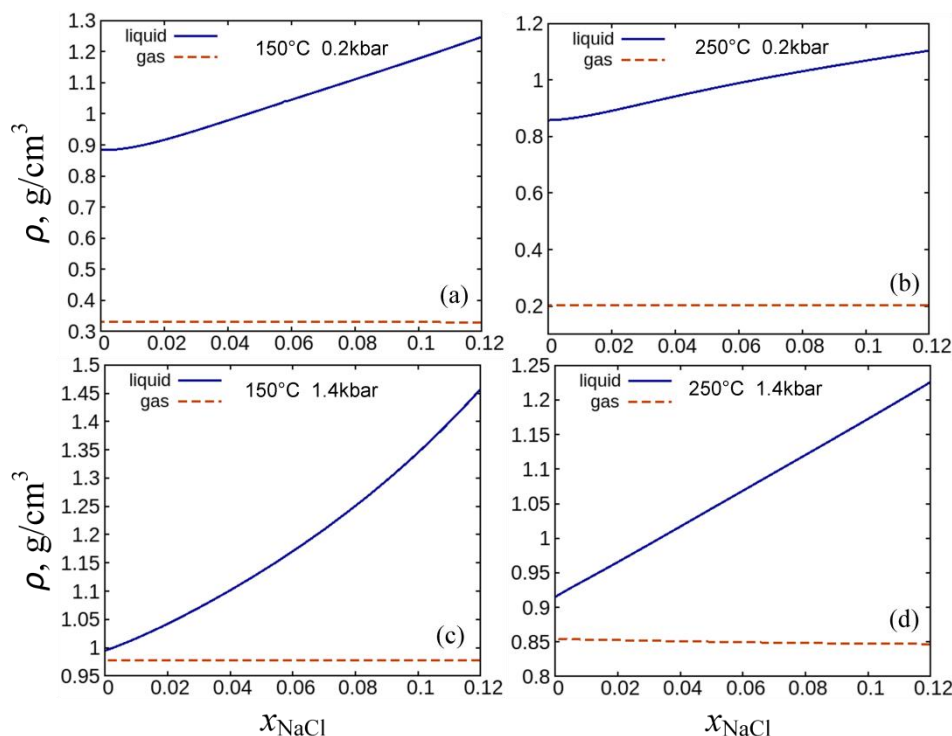


Figure 5. Densities of the liquid and gas phases on the solvus of the system $\text{H}_2\text{O}-\text{CO}_2-\text{NaCl}$ dependent on the mole fraction of NaCl.

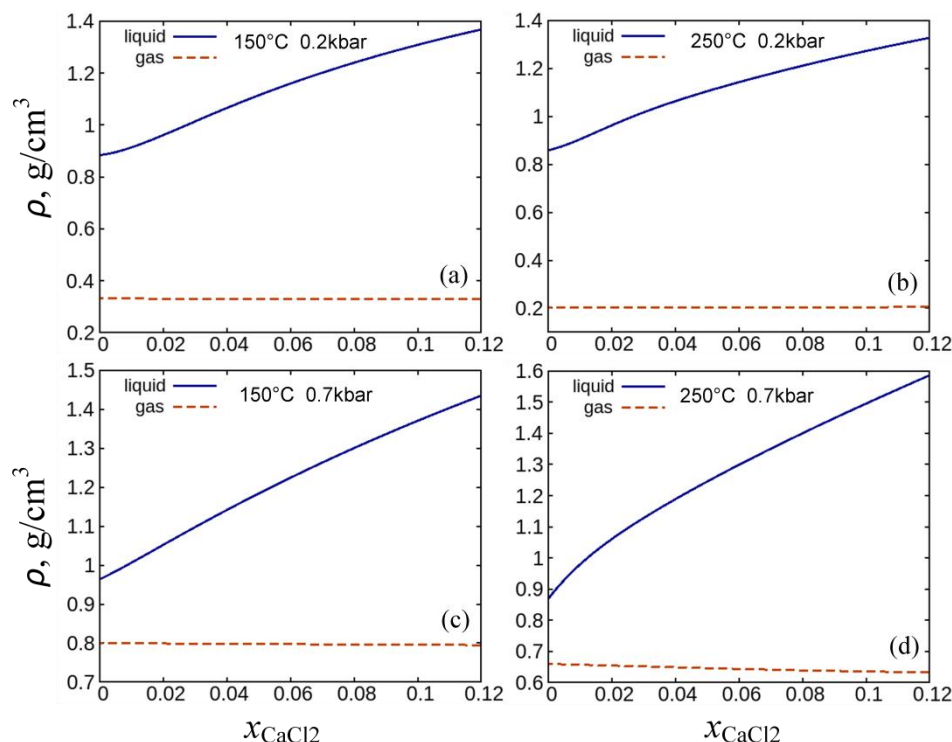


Figure 6. Densities of the liquid and gas phases on the solvus of the system $\text{H}_2\text{O}-\text{CO}_2-\text{CaCl}_2$ dependent on the mole fraction of CaCl_2 .

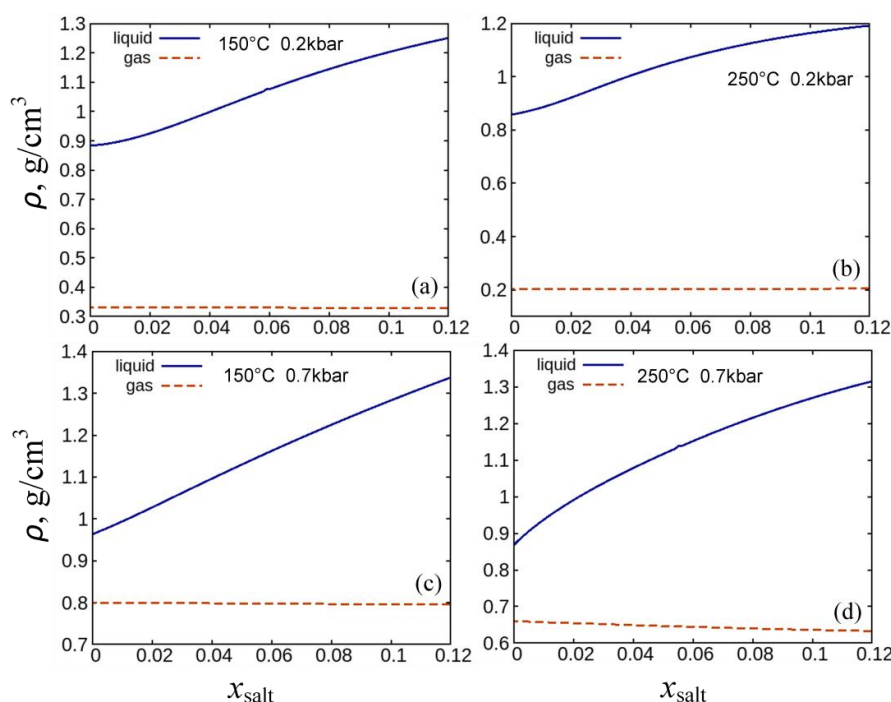


Figure 7. Densities of the liquid and gas phases on the solvus of the system $\text{H}_2\text{O}-\text{CO}_2-\text{NaCl}-\text{CaCl}_2$ dependent on the sum of mole fractions of NaCl and CaCl_2 x_{salt} when $x_{\text{NaCl}}:x_{\text{CaCl}_2} = 1:1$.

The P - T region studied above is associated with a number of metamorphic and metasomatic processes in the upper and middle crust, including formation of ore deposits of many non-ferrous and precious metals, such as Au, Ag, Cu, W, Mo, Pb, and so on. Fluid behavior, both in relation to ore occurrence and in the broader geological context, is a central question in many hundreds of studies. Examples include works [1,46–55] and recent studies [56–58]. The possibility of splitting aqueous fluids containing neutral gases into coexisting unmixable phases is an important factor in the precipitation of the solid phases from the fluid. The existing theoretical models for the P - T parameters considered on our paper are limited to a single $\text{H}_2\text{O}-\text{CO}_2-\text{NaCl}$ system. At the same time, the real geological fluids contain mixtures of several salts, in particular mixtures of NaCl and CaCl_2 [49,50,57]. A common way of avoiding this problem is combining all the salts in an “equivalent” concentration of NaCl, despite their different behavior in the nature [1,48–53,57–59]. Moreover, the available numerical models for the $\text{H}_2\text{O}-\text{CO}_2-\text{NaCl}$ system do not allow obtaining compositions of coexisting fluid phases, which is the central point in the analysis of fluid inclusions. As a result, the studies of the fluid inclusions do not have a reliable tool assessing the P - T parameters of phase separation of homogeneous fluids. The compositions

of the coexisting fluid phases correspond to the end points of the tie lines, similar to those shown in **Figure 3**. Phase diagrams and tie lines, similar to **Figure 3**, obtained from qualitative ideas without numerical thermodynamics, were presented in work [46]. These graphs were then repeated in some works [48,59], in connection with studies of fluid inclusions. Our thermodynamic model provides a reliable numerical basis for this type of the analysis of the fluid inclusions data. The computer program that performs calculations using the above model is available in the public domain [2].

The salinity of the deep fluids is often rather high [53–56] and significantly exceeds the limit of about 6 mol/kg characteristic of existing thermodynamic models of the $\text{H}_2\text{O}-\text{CO}_2-\text{NaCl}$ system. The models presented above are free from this limitation.

4. Conclusion

1. For the fluid system $\text{H}_2\text{O}-\text{CO}_2-\text{NaCl}$, a numerical thermodynamic model based on experimental data, and valid for pressures of 0.2–1.4 kbar and temperatures 150–300 °C, is developed. The model is valid for arbitrary concentrations of the components.
2. For the fluid system $\text{H}_2\text{O}-\text{CO}_2-\text{CaCl}_2$, a numerical ther-

modynamic model based on experimental data and valid for pressures of 0.2–0.7 kbar and temperatures 150–350 °C is developed. The model is valid for arbitrary concentrations of the components.

3. For the mixed aqueous solution H_2O -NaCl- CaCl_2 , a numerical thermodynamic model based on experimental data and valid for pressures of 0.2–0.7 kbar and temperatures 150–300 °C is developed. The model is valid for arbitrary concentrations of the components.
4. It is shown that affinity of CO_2 for NaCl is larger than the affinity of CO_2 for CaCl_2 in the subcritical P - T region considered in this paper. Together with the analogous conclusion on the affinity of CO_2 for NaCl and CaCl_2 done by us in work^[23] for the supercritical conditions, this allows to suppose that this difference in the affinity of CO_2 for NaCl and CaCl_2 is a general property of the aqueous fluids, independent on their P - T regime, both sub- and supercritical.
5. For the quaternary fluid system H_2O - CO_2 -NaCl- CaCl_2 , a numerical thermodynamic model based on models for three ternary edge systems and a proper form of the entropy of mixing is developed. The model is valid for pressures of 0.2–0.7 kbar, temperatures 150–300 °C, and for arbitrary concentrations of the components.
6. The developed models enable to predict the physicochemical properties of the fluid involved in the hydrothermal processes in the upper crust: the phase state of the system (homogeneous or two-phase fluid), position of the solvus separating the fields of the homogeneous and two-phase fluid, activities of the components, densities, and compositions of the (coexisting) fluid phases.
7. A set of phase diagrams for H_2O - CO_2 -NaCl, H_2O - CO_2 - CaCl_2 , and a quasi-ternary system H_2O - CO_2 -salt with $x_{\text{salt}} = x_{\text{NaCl}} + x_{\text{CaCl}_2}$ and a fixed ratio $x_{\text{NaCl}}/x_{\text{salt}} = 0.5$ is obtained for various P - T conditions. The largest fields of the homogeneous fluid correspond to the H_2O - CO_2 -NaCl system, the smallest ones to H_2O - CO_2 - CaCl_2 . The solvuses for quaternary systems with the mixed salt compositions lie between solvuses for these edge systems.
8. Tie lines connecting points of compositions of coexisting liquid and gas phases are plotted for a set of phase diagrams for H_2O - CO_2 -NaCl, H_2O - CO_2 - CaCl_2 , and the intermediate system with $x_{\text{NaCl}}/x_{\text{salt}} = 0.5$. For all the systems, including the case of the mixed salt compositions, the tie lines are straight lines with constant activities of components and constant compositions of the coexisting fluid phases.
9. It was shown that the increase of the mole fraction of the salt in the liquid phase leads to a decrease in the mole fraction of water in the coexisting gas phase. As a result, the composition of the gas phase shifts towards to the pure CO_2 , and the gap between gas and liquid phases widens.
10. The dependence of the activity $a_{\text{H}_2\text{O}}$ of water on x_{salt} and the salt composition is studied. The presence of CaCl_2 in the composition of the salt results in a decrease in the activity of water. The dependence of $a_{\text{H}_2\text{O}}$ on the portion of CaCl_2 in the salt can be non-monotonous. The minimum of $a_{\text{H}_2\text{O}}$ can be reached at a mixed composition of the salt.
11. Dependences of the densities of liquid and gas phases on the mole fraction of the salt on the solvus are obtained. The study was carried out for a wide range of pressures, different temperatures, and compositions of the salt component. In all the cases, the density of the liquid phase is higher than the density of the gas phase. The difference between two densities is minimal at low temperatures, high pressures, and low mole fractions of the salt. The difference between the densities increases rapidly when these conditions are violated.
12. The most evident direction of the following study of thermodynamics of fluids H_2O - CO_2 -salt in the upper crust P - T conditions is modeling the thermodynamic behavior of salt-containing fluids in an intermediate region, where water and CO_2 are infinitely miscible and the interaction between water and salt in the quasi gas phase step by step transforms from practically no interaction to the strong interaction typical for water solutions of salts and for the dense supercritical fluids.

Supplementary Material

The chemical potentials of the components of the quaternary fluid system H_2O - CO_2 -NaCl- CaCl_2 in the liquid phase are

$$\begin{aligned}
 \mu_1 = & RT\{\ln x_1 - \ln(1 + x_3 + 2x_4)\} \\
 & + RTA_{12}A_{21} \frac{x_2 (A_{12}x_1^2 + 2A_{21}x_1x_2 + A_{21}x_2^2 - A_{12}x_1^3 - A_{21}x_1^2x_2 - A_{21}x_1x_2^2 - A_{12}x_1^2x_2)}{(A_{12}x_1 + A_{21}x_2)^2} \\
 & + \frac{1}{2}\{x_3^{1/2} \ln(1 + x_3^{1/2}/\varepsilon_3) - x_3/(\varepsilon_3 + x_3^{1/2})\}W_{a3} + \frac{1}{2}\{x_4^{1/2} \ln(1 + x_4^{1/2}/\varepsilon_4) - x_4/(\varepsilon_4 + x_4^{1/2})\}W_{a4} \\
 & + x_3(1 - x_1)W_{b3} + x_4(1 - x_1)W_{b4} + x_3^2(1 - 2x_1)W_{c3} + x_4^2(1 - 2x_1)W_{c4} - W_{34a}x_3x_4 \\
 & - x_2x_3(W_{23}x_2 + W_{32}x_3)/(x_2 + x_3) - x_2x_4(W_{24}x_2 + W_{42}x_4)/(x_2 + x_4) \\
 \mu_2 = & RT\{\ln x_2 - \ln(1 + x_3 + 2x_4)\} \\
 & + RTA_{12}A_{21} \frac{x_1 (A_{21}x_2^2 + 2A_{12}x_1x_2 + A_{12}x_1^2 - A_{21}x_2^3 - A_{12}x_1x_2^2 - A_{12}x_1^2x_2 - A_{21}x_1x_2^2)}{(A_{12}x_1 + A_{21}x_2)^2} \\
 & + \frac{1}{2}\{x_3^{1/2} \ln(1 + x_3^{1/2}/\varepsilon_3) - x_3/(\varepsilon_3 + x_3^{1/2})\}W_{a3} + \frac{1}{2}\{x_4^{1/2} \ln(1 + x_4^{1/2}/\varepsilon_4) - x_4/(\varepsilon_4 + x_4^{1/2})\}W_{a4} \\
 & - x_1x_3W_{b3} - x_1x_4W_{b4} - 2x_1x_3^2W_{c3} - 2x_1x_4^2W_{c4} - W_{34a}x_3x_4 + W_{23}x_2x_3(x_2 - x_2^2 - x_2x_3 + 2x_3)/(x_2 + x_3)^2 \\
 & + W_{32}x_3^2(-x_2^2 + x_3 - x_2x_3)/(x_2 + x_3)^2 + W_{24}x_2x_4(x_2 - x_2^2 - x_2x_4 + 2x_4)/(x_2 + x_4)^2 \\
 & + W_{42}x_4^2(-x_2^2 + x_4 - x_2x_4)/(x_2 + x_4)^2 \\
 \mu_3 = & RT\{\ln x_3 + \ln(x_3 + 2x_4) - 2\ln(1 + x_3 + 2x_4)\} \\
 & + RTA_{12}A_{21} \frac{x_1x_2(x_1 + x_2)}{A_{12}x_1 + A_{21}x_2} + \left\{ \frac{1 + x_3}{2x_3^{1/2}} \ln(1 + x_3^{1/2}/\varepsilon_3) + \frac{1 - x_3}{2(\varepsilon_3 + x_3^{1/2})} - \ln(1 + 1/\varepsilon_3) \right\} W_{a3} \\
 & + \frac{1}{2} \left\{ x_4^{1/2} \ln(1 + x_4^{1/2}/\varepsilon_4) - x_4/(\varepsilon_4 + x_4^{1/2}) \right\} W_{a4} + x_1(1 - x_3)W_{b3} - x_1x_4W_{b4} + 2x_1x_3(1 - x_3)W_{c3} \\
 & - 2x_1x_4^2W_{c4} + W_{34a}(1 - x_3)x_4 + W_{23}x_2^2(x_2 - x_2x_3 - x_3^2)/(x_2 + x_3)^2 \\
 & + W_{32}x_2x_3(2x_2 + x_3 - x_3^2 - x_2x_3)/(x_2 + x_3)^2 - W_{24}x_2^2x_4/(x_2 + x_4) - W_{42}x_2x_4^2/(x_2 + x_4) \\
 \mu_4 = & RT\{\ln x_4 + 2\ln(x_3 + 2x_4) - 3\ln(1 + x_3 + 2x_4)\} + RTA_{12}A_{21} \frac{x_1x_2(x_1 + x_2)}{A_{12}x_1 + A_{21}x_2} \\
 & + \frac{1}{2} \left\{ x_3^{1/2} \ln(1 + x_3^{1/2}/\varepsilon_3) - x_3/(\varepsilon_3 + x_3^{1/2}) \right\} W_{a3} \\
 & + \left\{ \frac{1 + x_4}{2x_4^{1/2}} \ln(1 + x_4^{1/2}/\varepsilon_4) + \frac{1 - x_4}{2(\varepsilon_4 + x_4^{1/2})} - \ln(1 + 1/\varepsilon_4) \right\} W_{a4} + x_1(1 - x_4)W_{b4} - x_1x_3W_{b3} \\
 & - 2x_1x_3^2W_{c3} + 2x_1x_4(1 - x_4)W_{c4} + W_{34a}(1 - x_4)x_3 + W_{24}x_2^2(x_2 - x_2x_4 - x_4^2)/(x_2 + x_4)^2 \\
 & + W_{42}x_2x_4(2x_2 + x_4 - x_4^2 - x_2x_4)/(x_2 + x_4)^2 - W_{23}x_2^2x_3/(x_2 + x_3) - W_{32}x_2x_3^2/(x_2 + x_3)
 \end{aligned}$$

The chemical potentials of the pure components, μ_{i0} i.e. for $x_i = 1$ are equal to zero

$$\mu_{10} = \mu_{20} = \mu_{30} = \mu_{40} = 0$$

Activities of H₂O and CO₂ can be calculated by the general formulas

$$a_i = \exp\left(\frac{\mu_i - \mu_{i0}}{RT}\right)$$

The same formulas can be applied for the activity of

NaCl in ternary system H₂O-CO₂-NaCl and activity of CaCl₂ in H₂O-CO₂-CaCl₂. The calculation of activities of NaCl and CaCl₂ in the systems with two salts does not make sense because these salts do not exist in the aqueous phase as separate compounds.

Funding

The study was conducted under the Research Program of the IPGG RAS FMUW-2021-0002. The computational

part of the work was made on the equipment of the Shared Equipment Center AIRES (Analytical Investigation of the Rising Earth Story) of the IPGG RAS.

Institutional Review Board Statement

Not applicable.

Informed Consent Statement

Not applicable.

Data Availability Statement

The experimental data used in the study are available in the cited publications. A computer program that performs calculations of phase diagrams and solvuses according to the presented thermodynamic models is available in the public domain. Ivanov, M.V., 2025. Program H2OCO2NaClCaCl2_Low_T. Available from: <https://www.dropbox.com/scl/fo/b1nknqygjg2dx4zd2j8ze/AF10zN1INwJtF62O31e9r4?rlkey=v1klz1e1c6p07z8h33accpeu&st=qv150af7&dl=0>.

Conflict of Interest

The author declares that there is no conflict of interest.

References

- [1] Williams-Jones, A.E., Heinrich, C.A., 2005. Vapor Transport of Metals and the Formation of Magmatic-Hydrothermal Ore Deposits. *Economic Geology*. 100(7), 1287–1312. DOI: <https://doi.org/10.2113/gsecongeo.100.7.1287>
- [2] Heinrich, W., 2007. Fluid Immiscibility in Metamorphic Rocks. *Reviews in Mineralogy and Geochemistry*. 65(1), 389–430. DOI: <https://doi.org/10.2138/rmg.2007.65.12>
- [3] Fu, B., Touret, J.L.R., 2014. From Granulite Fluids to Quartz-Carbonate Megashear Zones: The Gold Rush. *Geoscience Frontiers*. 5(5), 747–758. DOI: <https://doi.org/10.1016/j.gsf.2014.03.013>
- [4] Li, Y., Ngheim, L.X., 1986. Phase Equilibria of Oil, Gas and Water/Brine Mixtures from a Cubic Equation of State and Henry's Law. *Canadian Journal of Chemical Engineering*. 64(3), 486–496. DOI: <https://doi.org/10.1002/cjce.5450640319>
- [5] Duan, Z., Sun, R., 2003. An Improved Model Calculating CO₂ Solubility in Pure Water and Aqueous NaCl Solutions from 273 to 533 K and from 0 to 2000 Bar. *Chemical Geology*. 193(3–4), 257–271. DOI: [https://doi.org/10.1016/S0009-2541\(02\)00263-2](https://doi.org/10.1016/S0009-2541(02)00263-2)
- [6] Papaiconomou, N., Simonin, J.P., Bernard, O., et al., 2003. Description of Vapor-Liquid Equilibria for CO₂ in Electrolyte Solutions Using the Mean Spherical Approximation. *The Journal of Physical Chemistry B*. 107(24), 5948–5957. DOI: <https://doi.org/10.1021/jp034294x>
- [7] Spycher, N., Pruess, K., 2005. CO₂-H₂O Mixtures in the Geological Sequestration of CO₂. II. Partitioning in Chloride Brines at 12–100°C and up to 600 Bar. *Geochimica et Cosmochimica Acta*. 69(13), 3309–3320. DOI: <https://doi.org/10.1016/j.gca.2005.01.015>
- [8] Duan, Z., Hu, J., Li, D., et al., 2008. Densities of the CO₂-H₂O and CO₂-H₂O-NaCl Systems up to 647 K and 100 MPa. *Energy and Fuels*. 22(3), 1666–1674. DOI: <https://doi.org/10.1021/ef700666b>
- [9] Akinfiev, N.N., Diamond, L.W., 2010. Thermodynamic Model of Aqueous CO₂-H₂O-NaCl Solutions from –22 to 100°C and from 0.1 to 100 MPa. *Fluid Phase Equilibria*. 295(1), 104–124. DOI: <https://doi.org/10.1016/j.fluid.2010.04.007>
- [10] Sun, R., Dubessy, J., 2012. Prediction of Vapor-Liquid Equilibrium and PVTx Properties of Geological Fluid System with SAFT-LJ EOS Including Multi-Polar Contribution. Part II: Application to H₂O-NaCl and H₂O-CO₂-NaCl System. *Geochimica et Cosmochimica Acta*. 88(1), 130–145. DOI: <https://doi.org/10.1016/j.gca.2012.04.025>
- [11] Dubacq, B., Bickle, M.J., Evans, K.A., 2013. An Activity Model for Phase Equilibria in the H₂O-CO₂-NaCl System. *Geochimica et Cosmochimica Acta*. 110, 229–252. DOI: <https://doi.org/10.1016/j.gca.2013.02.008>
- [12] Mao, S., Hu, J., Zhang, Y., et al., 2015. A Predictive Model for the PVTx Properties of CO₂-H₂O-NaCl Fluid Mixture up to High Temperature and High Pressure. *Applied Geochemistry*. 54, 54–64. DOI: <https://doi.org/10.1016/j.apgeochem.2015.01.003>
- [13] Bain, X.Q., Xiong, W., Kasthuriarchchi, D.T.K., et al., 2019. Phase Equilibrium Modeling for Carbon Dioxide Solubility in Aqueous Sodium Chloride Solutions Using an Association Equation of State. *Industrial and Engineering Chemistry Research*. 58(24), 10570–10578. DOI: <https://doi.org/10.1021/acs.iecr.9b01736>
- [14] Pitzer, K.S., Peiper, J.C., Busey, R.H., 1984. Thermodynamic Properties of Aqueous Sodium Chloride Solutions. *Journal of Physical and Chemical Reference Data*. 13, 1–102. DOI: <https://doi.org/10.1063/1.555709>
- [15] Archer, D.G., 1992. Thermodynamic Properties of the NaCl+H₂O System. II. Thermodynamic Proper-

- ties of NaCl(aq), NaCl·2H₂(cr), and Phase Equilibria. *Journal of Physical and Chemical Reference Data*. 21, 793–829. DOI: <https://doi.org/10.1063/1.555915>
- [16] Ivanov, M.V., Bushmin, S.A., Aranovich, L.Y., 2018. An Empirical Model of the Gibbs Free Energy for Solutions of NaCl and CaCl₂ of Arbitrary Concentration at Temperatures from 423.15 K to 623.15 K under Vapor Saturation Pressure. *Doklady Earth Sciences*. 479, 491–494. DOI: <https://doi.org/10.1134/S1028334X18040141>
- [17] Zhang, Y.G., Frantz, J.D., 1989. Experimental Determination of the Compositional Limits of Immiscibility in the System CaCl₂-H₂O-CO₂ at High Temperatures and Pressures Using Synthetic Fluid Inclusions. *Chemical Geology*. 74(3–4), 289–308. DOI: [https://doi.org/10.1016/0009-2541\(89\)90039-9](https://doi.org/10.1016/0009-2541(89)90039-9)
- [18] Shmulovich, K.I., Plyasunova, N.V., 1993. High-Temperature High-Pressure Phase Equilibria in the Ternary System H₂O-CO₂-Salt (CaCl₂, NaCl). *Geokhimiya*. 5, 666–684.
- [19] Shmulovich, K.I., Graham, C.M., 2004. An Experimental Study of Phase Equilibria in the Systems H₂O-CO₂-CaCl₂ and H₂O-O₂-NaCl at High Pressures and Temperatures (500–800°C, 0.5–0.9 GPa): Geological and Geophysical Applications. *Contributions to Mineralogy and Petrology*. 146, 450–462. DOI: <https://doi.org/10.1007/s00410-003-0507-5>
- [20] Ivanov, M.V., Bushmin, S.A., 2019. Equation of State of the Fluid System H₂O-CO₂-CaCl₂ and Properties of Fluid Phases at P–T Parameters of the Middle and Lower Crust. *Petrology*. 27, 395–406. DOI: <https://doi.org/10.1134/S0869591119040039>
- [21] Bischoff, J.L., Rosenbauer, R.J., Fournier, R.O., 1996. The Generation of HCl in the System CaCl₂-H₂O: Vapor-Liquid Relations from 380–500°C. *Geochimica et Cosmochimica Acta*. 60(1), 7–16. DOI: [https://doi.org/10.1016/0016-7037\(95\)00365-7](https://doi.org/10.1016/0016-7037(95)00365-7)
- [22] Ivanov, M.V., 2023. Thermodynamic Model of the Fluid System H₂O-CO₂-NaCl-CaCl₂ at P–T Parameters of the Middle and Lower Crust. *Petrology*. 31, 413–423. DOI: <https://doi.org/10.1134/S0869591123040045>
- [23] Ivanov, M.V., Bushmin, S.A., 2024. Separation of Salts NaCl and CaCl₂ in Aqueous–Carbon Dioxide Deep Fluids. *Petrology*. 32, 249–257. DOI: <https://doi.org/10.1134/S0869591124020036>
- [24] Aranovich, L.Ya., Zakirov, I.V., Sretenskaya, N.G., et al., 2010. Ternary System H₂O-CO₂-NaCl at High T–P Parameters: An Empirical Mixing Model. *Geochemistry International*. 48, 446–455. DOI: <https://doi.org/10.1134/S0016702910050022>
- [25] Ivanov, M.V., Bushmin, S.A., 2021. Thermodynamic Model of the Fluid System H₂O-CO₂-NaCl at P–T Parameters of the Middle and Lower Crust. *Petrology*. 29, 77–88. DOI: <https://doi.org/10.1134/S086959112006003X>
- [26] Ivanov, M.V., Bushmin, S.A., Aranovich, L.Y., 2018. Equations of State for NaCl and CaCl₂ Solutions of Arbitrary Concentration at Temperatures 423.15–623.15 K and Pressures up to 5 kbar. *Doklady Earth Sciences*. 481, 1086–1090. DOI: <https://doi.org/10.1134/S1028334X18080287>
- [27] Atkins, P., de Paula, J., 2009. *Elements of Physical Chemistry*. Oxford University Press: Oxford, UK.
- [28] Ivanov, M.V., Babikov, D., 2011. Collisional Stabilization of Van der Waals States of Ozone. *Journal of Chemical Physics*. 134, 174308. DOI: <https://doi.org/10.1063/1.3585690>
- [29] Ivanov, M.V., Babikov, D., 2012. Efficient Quantum–Classical Method for Computing Thermal Rate Constant of Recombination: Application to Ozone Formation. *Journal of Chemical Physics*. 136, 184304. DOI: <https://doi.org/10.1063/1.4711760>
- [30] Ivanov, M.V., Babikov, D., 2013. On Molecular Origin of Mass-Independent Fractionation of Oxygen Isotopes in the Ozone Forming Recombination Reaction. *PNAS*. 110(44), 17708–17713. DOI: <https://doi.org/10.1073/pnas.1215464110>
- [31] Semenov, A., Ivanov, M., Babikov, D., 2013. Rotational Quenching of CO (v = 1) by He Impact in a Broad Range of Temperatures: A Benchmark Study Using Mixed Quantum/Classical Inelastic Scattering Theory. *Journal of Chemical Physics*. 139, 074306. DOI: <https://doi.org/10.1063/1.4818488>
- [32] Ivanov, M.V., Babikov, D., 2016. On Stabilization of Scattering Resonances in Recombination Reaction That Forms Ozone. *Journal of Chemical Physics*. 144, 154301. DOI: <https://doi.org/10.1063/1.4945779>
- [33] Zevin, D., Driesner, T., Scott, S., et al., 2014. Volumetric Properties of Mixed Aqueous Solutions at Elevated Temperatures and Pressures: The Systems CaCl₂-NaCl-H₂O and MgCl₂-NaCl-H₂O to 523.15 K, 70 MPa, and Ionic Strength from 0.1 to 18 mol·kg⁻¹. *Journal of Chemical & Engineering Data*. 59(8), 2570–2588. DOI: <https://doi.org/10.1021/je500371u>
- [34] Wagner, W., Prüss, A., 2002. The IAPWS Formulation 1995 for the Thermodynamic Properties of Ordinary Water Substance for General and Scientific Use. *Journal of Physical and Chemical Reference Data*. 31, 387–535. DOI: <https://doi.org/10.1063/1.1461829>
- [35] Span, R., Wagner, W., 1996. A New Equation of State for Carbon Dioxide Covering the Fluid Region from the Triple-Point Temperature to 1100 K at Pressures up to 800 MPa. *Journal of Physical and Chemical Reference Data*. 25, 1509–1596. DOI: <https://doi.org/10.1063/1.555991>
- [36] Ivanov, M.V., 2025. Equation of State of a Fluid H₂O-CO₂ at Temperatures 50–350°C and Pressures 0.2–3.5 kbar. *Journal of Environmental and Earth Sciences*. 7(1), 625–631. DOI: <https://doi.org/10.30564/jees.v>

- 7i1.7327
- [37] Tödheide, K., Franck, E.U., 1963. The Two-Phase Region and the Critical Curve in the Carbon Dioxide–Water System up to Pressure of 3500 Bar. *Zeitschrift für Physikalische Chemie Neue Folge*. 37(5–6), 387–401. DOI: <https://doi.org/10.1524/zpch.1963.37.5.6.387>
- [38] Sourirajan, S., Kennedy, G.C., 1962. The System H₂O–NaCl at Elevated Temperatures and Pressures. *American Journal of Science*. 260(2), 115–141. DOI: <https://doi.org/10.2475/ajs.260.2.115>
- [39] Driesner, T., Heinrich, C.A., 2007. The System H₂O–NaCl. Part I: Correlation Formulae for Phase Relations in Temperature–Pressure–Composition Space from 0 to 1000°C, 0 to 5000 Bar, and 0 to 1 XNaCl. *Geochimica et Cosmochimica Acta*. 71(20), 4880–4901. DOI: <https://doi.org/10.1016/j.gca.2006.01.033>
- [40] Ellingsen, L., Haug-Warberg, T., 2024. Thermodynamics of NaCl in Dense Water Vapor via Cross Virial Coefficients. *Geochimica et Cosmochimica Acta*. 375, 19–35. DOI: <https://doi.org/10.1016/j.gca.2024.04.033>
- [41] Chase, M.W., 1988. NIST-JANAF Thermochemical Tables. American Chemical Society/American Institute of Physics for the National Bureau of Standards: Washington, DC, USA.
- [42] Zakirov, I., Sretenskaja, N., Aranovich, L., et al., 2007. Solubility of NaCl in CO₂ at High Pressure and Temperature: First Experimental Measurements. *Geochimica et Cosmochimica Acta*. 71(17), 4251–4255. DOI: <http://doi.org/10.1016/j.gca.2007.01.028>
- [43] Takenouchi, S., Kennedy, G.C., 1965. The Solubility of Carbon Dioxide in NaCl Solutions at High Temperatures and Pressures. *American Journal of Science*. 263(5), 445–454. DOI: <https://doi.org/10.2475/AJS.263.5.445>
- [44] Malinin, S.D., 1959. System Water–Carbon Dioxide at High Temperatures and Pressures. *Geokhimiya*. 3, 235–245.
- [45] Malinin, S.D., 1979. Physical Chemistry of Hydrothermal Systems: The Carbon Dioxide. Nauka Publishing: Moscow, Russia. (in Russian)
- [46] Pichavant, M., Ramboz, C., Weisbrod, A., 1982. Fluid Immiscibility in Natural Processes: Use and Misuse of Fluid Inclusion Data, I. Phase Equilibria Analysis – A Theoretical and Geometrical Approach. *Chemical Geology*. 37(1–2), 1–27. DOI: [https://doi.org/10.1016/0009-2541\(82\)90064-X](https://doi.org/10.1016/0009-2541(82)90064-X)
- [47] Ramboz, C., Pichavant, M., Weisbrod, A., 1982. Fluid Immiscibility in Natural Processes: Use and Misuse of Fluid Inclusion Data, II. Interpretation of Fluid Inclusion Data in Terms of Immiscibility. *Chemical Geology*. 37(1–2), 29–48. DOI: [https://doi.org/10.1016/0009-2541\(82\)90065-1](https://doi.org/10.1016/0009-2541(82)90065-1)
- [48] Dugdale, A.L., Hagemann, S.G., 2001. The Bronzewing Lode-Gold Deposit, Western Australia: P–T–X Evidence for Fluid Immiscibility Caused by Cyclic Decompression in Gold-Bearing Quartz Veins. *Chemical Geology*. 173(1–3), 59–90. DOI: [https://doi.org/10.1016/S0009-2541\(00\)00268-0](https://doi.org/10.1016/S0009-2541(00)00268-0)
- [49] Bons, P.D., Elburg, M.A., Gomez-Rivas, E., 2012. A Review of the Formation of Tectonic Veins and Their Microstructures. *Journal of Structural Geology*. 43, 33–62. DOI: <https://doi.org/10.1016/j.jsg.2012.07.005>
- [50] Etheridge, M.A., Wall, V.J., Vernon, R.H., 1983. The Role of the Fluid Phase During Regional Metamorphism and Deformation. *Journal of Metamorphic Geology*. 1(3), 205–226. DOI: <https://doi.org/10.1111/j.1525-1314.1983.tb00272.x>
- [51] Marsala, A., Wagner, T., 2016. Mass Transfer and Fluid Evolution in Late-Metamorphic Veins, Rhenish Massif (Germany): Insight from Alteration Geochemistry and Fluid–Mineral Equilibria Modeling. *Mineralogy and Petrology*. 110, 515–545. DOI: <https://doi.org/10.1007/s00710-016-0424-8>
- [52] Asadi, S., Moore, F., 2017. Fluid Evolution in H₂O–CO₂–NaCl System and Metallogenic Analysis of the Surian Metamorphic Complex, Bavanat Cu Deposit, Southwest Iran. *Mineralogy and Petrology*. 111, 145–161. DOI: <https://doi.org/10.1007/s00710-016-0457-z>
- [53] Yardley, B.W.D., Graham, J.T., 2002. The Origins of Salinity in Metamorphic Fluids. *Geofluids*. 2, 249–256. DOI: <https://dx.doi.org/10.1046/j.1468-8123.2002.00042.x>
- [54] Aranovich, L.Y., Newton, R.C., Manning, C.E., 2013. Brine-Assisted Anatexis: Experimental Melting in the System Haplogranite–H₂O–NaCl–KCl at Deep-Crustal Conditions. *Earth and Planetary Science Letters*. 374, 111–120. DOI: <https://doi.org/10.1016/j.epsl.2013.05.027>
- [55] Aranovich, L.Y., Makhluif, A.R., Newton, R.C., et al., 2014. Dehydration Melting and the Relationship Between Granites and Granulites. *Precambrian Research*. 253, 26–37. DOI: <https://dx.doi.org/10.1016/j.precamres.2014.07.004>
- [56] Volkov, I.S., Kozlovskii, V.M., 2023. Formation Stages and Conditions of Carbonate–Silicate Veins and Their Wall-Rock Aureoles in the Early Proterozoic Complexes of the Belomorian Mobile Belt, Northern Karelia. *Petrology*. 31, 538–557. DOI: <https://doi.org/10.1134/S0869591123050077>
- [57] Volkov, I.S., Prokofiev, V.Y., Kozlovskii, V.M., et al., 2023. Sulfide Mineralization of Carbonate–Silicate Veins in Early Proterozoic Metabasites of North Karelia: Mineral Assemblages, Mineral Forms of Silver, and Fluid Inclusions. *Geology of Ore De-*

- posits. 65, 567–594. DOI: <https://doi.org/10.1134/S1075701523060107>
- [58] Volkov, I.S., Dubinina, E.O., Kossova, S.A., et al., 2024. Isotope ($\delta^{18}\text{O}$, $\delta^{13}\text{C}$, δD) Characteristics of Biotite–Carbonate–Quartz Associations of Hydrothermal Veins in Metabasites of North Karelia. *Doklady Earth Sciences*. 518, 1465–1471. DOI: <https://doi.org/10.1134/S10283334X24602566>
- [59] Volkov, I.S., 2024. Hydrothermal Veins in Metabasites of North Karelia: Mineral Associations, Formation Conditions and Fluid Composition [PhD Thesis]. Institute of the Geology of Ore Deposits, Petrography, Mineralogy, and Geochemistry, Russian Academy of Sciences: Moscow, Russia. pp. 1–128. (in Russian)